iScience

CellPress
OPEN ACCESS

Article

Functional remodeling of presynaptic voltage-gated calcium channels in superficial layers of the dorsal horn during neuropathic pain

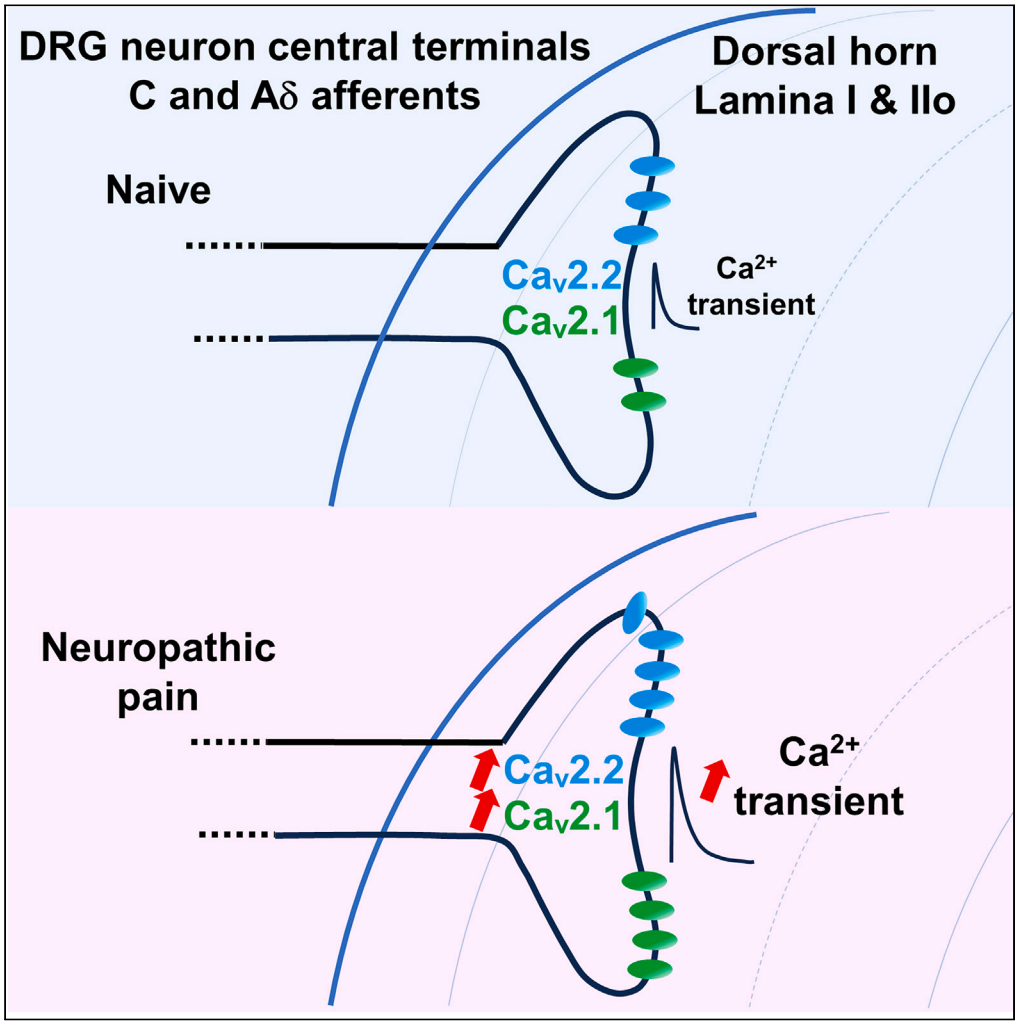

Laurent Ferron, Erika K. Harding, Maria A. Gandini, Craig Brideau, Peter K. Stys, Gerald W. Zamponi

zamponi@ucalgary.ca

Highlights

2-P Ca^{2+} imaging was done in nociceptor nerve terminals in *ex vivo* spinal cord

Synaptic Ca^{2+} transients in nociceptor synapses are increased during neuropathic pain

Nociceptor synaptic N- and P/Q-type channels are upregulated in neuropathic pain

GABA-B receptor inhibition of synaptic Ca^{2+} channels is enhanced during chronic pain

Ferron et al., iScience *27*, 109973
June 21, 2024
https://doi.org/10.1016/j.isci.2024.109973

iScience

CellPress
OPEN ACCESS

Article

Functional remodeling of presynaptic voltage-gated calcium channels in superficial layers of the dorsal horn during neuropathic pain

Laurent Ferron,[1] Erika K. Harding,[1] Maria A. Gandini,[1] Craig Brideau,[1] Peter K. Stys,[1] and Gerald W. Zamponi[1,2,*]

SUMMARY

N- and P/Q-type voltage-gated Ca^{2+} channels are critical for synaptic transmission. While their expression is increased in the dorsal root ganglion (DRG) neuron cell bodies during neuropathic pain conditions, less is known about their synaptic remodeling. Here, we combined genetic tools with 2-photon Ca^{2+} imaging to explore the functional remodeling that occurs in central presynaptic terminals of DRG neurons during neuropathic pain. We imaged GCaMP6s fluorescence responses in an *ex vivo* spinal cord preparation from mice expressing GCaMP6s in Trpv1-Cre lineage nociceptors. We show that Ca^{2+} transient amplitude is increased in central terminals of these neurons after spared nerve injury, and that this increase is mediated by both N- and P/Q-type channels. We found that GABA-B receptor-dependent inhibition of Ca^{2+} transients was potentiated in the superficial layer of the dorsal horn. Our results provide direct evidence toward nerve injury-induced functional remodeling of presynaptic Ca^{2+} channels in Trpv1-lineage nociceptor terminals.

INTRODUCTION

Voltage-gated calcium channels (Ca_V) are key modulators of neuronal excitability and synaptic transmission.[1,2] Among the three families of Ca_V, $Ca_V2.X$ family members, especially $Ca_V2.1$ (P/Q-type) and $Ca_V2.2$ (N-type), are pivotal in primary afferent neurotransmission in the spinal cord dorsal horn.[3] $Ca_V2.X$ channels are protein complexes composed of a pore forming $Ca_V\alpha1$ subunit and auxiliary $Ca_V\beta$ and $Ca_V\alpha2\text{-}\delta$ subunits that play critical roles in the trafficking of the channel.[4–6] N-type channels and the $Ca_V\alpha2\text{-}\delta1$ auxiliary subunit are validated pharmacological targets for treating pain.[7,8] Indeed, $Ca_V\alpha2\text{-}\delta1$ is the dominant isoform expressed in DRG neurons and is upregulated in models of chronic pain.[9–11] Gabapentinoids, which are used to treat neuropathic pain, target $Ca_V\alpha2\text{-}\delta1$ and dampen the trafficking of $Ca_V2.2$ channels.[12–14] Moreover, specific peptide blockers for N-type channels, such as ω-conotoxin-GVIA (GVIA), have been instrumental in demonstrating their involvement in the afferent pain pathway and they are now used to treat severe chronic pain.[15,16]

Chronic pain is characterized by an increase in excitability of the primary afferents.[17–20] This alteration of neuronal excitability results from the dysregulation of ion channel expression including that of Ca_V channels in these cells. In the chronic pain context, increases in protein levels of $Ca_V2.1$ and $Ca_V2.2$ channels and their contribution to postsynaptic responses have been reported in dorsal root ganglia (DRG) and in the spinal cord.[21–26] However, it is still not clear whether the increase of $Ca_V2.X$ channels in the dorsal horn results from an increase in the trafficking of channels from the DRG into their central terminals or an increase of channels in spinal neurons, or a combination of both mechanisms. Moreover, functional alterations in Ca^{2+} channel activity in chronic pain states in intact preparations which preserve the architecture of the spinal cord have not been verified.

Typically, activity in presynaptic terminals from primary afferent fibers is indirectly monitored by electrophysiological recordings from somata of postsynaptic neurons in spinal cord slices,[3,27–32] and Ca^{2+} imaging has been used effectively in such preparations.[33] In contrast, direct access to Ca^{2+} signaling in presynaptic nerve terminals in *ex vivo* preparations has been difficult. Indeed, the spinal cord is covered with nerve tracts formed by myelinated fibers and dorsal root entry zones are also heavily myelinated structures. Myelin scatters light which makes optical imaging of dorsal horn neuronal compartments challenging.[34] However, recent developments in 2-photon Ca^{2+} imaging, using either bulk loading of synthetic Ca^{2+} indicators into neuronal tissue or transgenic mice expressing genetically encoded Ca^{2+} indicators, have enabled the investigation of spinal neuron activity in the superficial layers of the dorsal horn with cellular resolution.[35–37]

Here we used transgenic animals in combination with 2-photon imaging to directly explore the functional remodeling of Ca_V channels in DRG neuron presynaptic terminals in an *ex vivo* spinal dorsal horn preparation during a chronic pain state. By crossing a Trpv1-Cre mouse line with a cre-dependent GCaMP6s reporter mouse line, we restricted the expression of the genetically encoded Ca^{2+} indicator to nociceptors in the peripheral nervous system and to very few neurons in the central nervous system, especially in the dorsal horn.[38] This latter point was crucial as it allowed us to image DRG central terminals at subcellular resolution, without contamination by somata or dendrites from spinal

[1]Department of Clinical Neurosciences, Hotchkiss Brain Institute, Calgary Cumming School of Medicine, University of Calgary, 3330 Hospital Drive NW, Calgary, Alberta T2N 4N1, Canada
[2]Lead contact
*Correspondence: zamponi@ucalgary.ca
https://doi.org/10.1016/j.isci.2024.109973

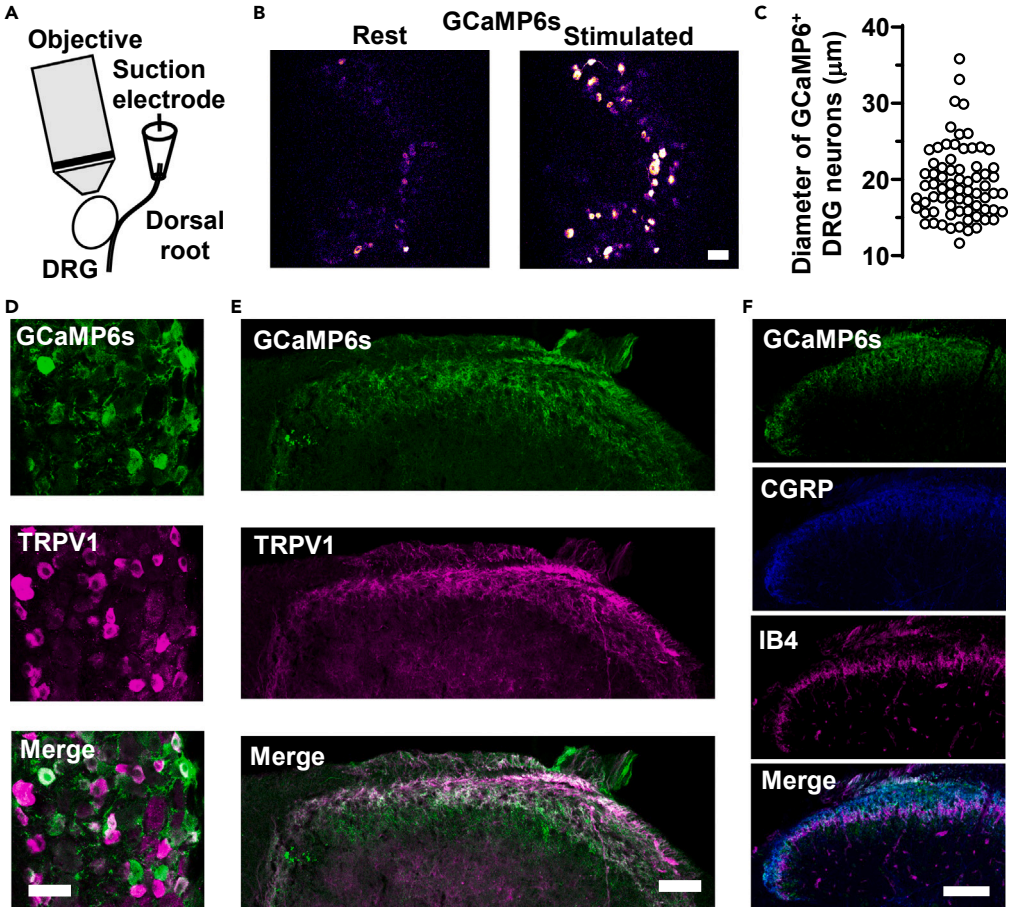

Figure 1. Expression profile for GCaMP6s and Trpv1 in DRG and dorsal spinal cord of Trpv1-Cre mice crossed with Ai96 mice

(A) Schematic of the dorsal root ganglion (DRG) imaging setup and dorsal root stimulation.

(B) Two-photon images of an L4 dorsal root ganglion from a Trvp1-CrexAi96 mouse at rest (left panel) and during stimulation (2 mA for 5 s, right panel). DRG neurons were stimulated via the dorsal root using a suction electrode. Scale bar: 50 μm.

(C) Plot showing the diameter of soma of DRG neurons expressing GCaMP6s (n = 71 neurons from 3 L4 ganglia).

(D) Confocal images of GCaMP6s and Trpv1 expression in L4 DRG of a Trpv1-Cre x Ai96 mouse. DRG sections were immunostained with GFP Ab (stains GCaMP6s—green) and Trpv1 Ab (magenta). The merged image shows a portion of GCaMP6s positive neurons lacking staining for Trpv1 (bottom panel). Scale bar: 50 μm.

(E) Confocal images of GCaMP6s and Trpv1 expression in superficial layers of the dorsal horn of a Trpv1-Cre x Ai96 mouse (L4–L5). Lumbar sections of the spinal cord (L4 to L5) were immunostained with GFP Ab (stains GCaMP6s—green) and Trpv1 Ab (magenta). The merged image indicates GCaMP6s and Trpv1 co-expression in superficial layers of the dorsal horn (bottom panel). Scale bar: 50 μm.

(F) Confocal images of GCaMP6s expression in superficial layers of the dorsal horn of a Trpv1-Cre x Ai96 mouse (L4–L5). Lumbar sections of the spinal cord (L4 to L5) were immunostained with GFP Ab (stains GCaMP6s (green), CGRP Ab (blue), and IB4-AF647 (magenta)). The merged image reveals expression of GCaMP6s in CGRP-positive layer and to a less extend IB4-positive layer (bottom panel). Scale bar: 100 μm.

cord neurons. We were thus able to demonstrate specific functional alterations in Ca^{2+} channel mediated presynaptic Ca^{2+} signals in primary afferent nerve terminals in the intact spinal cord in response to peripheral nerve injury.

RESULTS

SNI increases Ca^{2+} transient amplitude in Trpv1-lineage L4 DRG neuron central terminals in response to a sustained stimulation

To test the hypothesis that spared nerve injury (SNI) alters Ca^{2+} activity in DRG neuron central terminals, we monitored the responses of nociceptors to stimulation using 2-photon Ca^{2+} imaging. The genetically encoded Ca^{2+} indicator GCaMP6s was specifically expressed in a subset of nociceptors by crossing the Trpv1-Cre driver mouse line with the Ai96 conditional allele mice.[38] To confirm the expression of GCaMP6s in DRG neuron somata, we isolated dorsal root ganglia containing the dorsal root, stimulated the dorsal root with a suction electrode, and imaged the ganglia using a 2-photon microscope (Figures 1A and 1B). We found that the diameter of DRG neurons expressing GCaMP6s

varied from 13 to 35 μm, with 52% <20 μm and 38% between 20 and 25 μm (Figure 1C), which correspond to small and medium DRG neurons.[39] This result is consistent with previous reports describing small-diameter, unmyelinated C-fibers and medium-diameter, thinly myelinated Aδ fibers expressing Trpv1 in DRGs.[28,38,40] We performed immunohistochemistry staining on sections of L4 DRG (Figure 1D), revealing that 63 ± 4% (n = 5) of GCaMP6s positive DRG neuron cell bodies were immuno-positive for Trpv1 channels. We also performed staining on spinal cord sections (Figure 1E) revealing that Trpv1 channels were highly expressed in DRG terminals in superficial layers of the dorsal spinal cord. When comparing Trpv1 staining with GCaMP6 staining in the spinal cord, we observed that GCaMP6 staining from DRG terminals penetrated slightly deeper layers of the dorsal horn. The superficial layers that were Trpv1 and GCaMP6 positive were also CGRP positive (Figure 1F, lamina [LI] I and lamina II outer [LIIo]) and the deeper layers that were mostly GCaMP6 positive were also IB4 positive (Figure 1F, lamina II inner and LIIo).[41] Overall, our data are in line with the conclusions of the initial studies performed on this Trpv1-Cre mouse line.[38,42] During development, Trpv1 is transiently expressed in several DRG neuron subtypes including both prospective peptidergic and nonpeptidergic neurons.[42] The consequence for our study is that, when we imaged GCaMP6s positive terminals in the spinal dorsal horn, we imaged Trpv1 lineage neuron terminals rather than Trpv1 positive neuron terminals, and a fraction of these neuron terminals are likely not Trpv1 positive in adult mice, especially in deeper layers of the dorsal horn. We thus refer to GCaMP6 expressing neurons as Trpv1 lineage neurons (abbreviated as Trpv1$^+$).

We then focused on the central terminals of DRG neurons expressing GCaMP6s (Trpv1$^+$). We isolated the whole lumbar spinal cord of Trpv1-GCaMP6s mice with dorsal roots attached. The left L4 dorsal root was connected with a suction electrode to a stimulator (Figure 2A). We imaged the lateral left dorsal horn (ipsilateral side, at the level of the dorsolateral fasciculus) between L4 and L5 dorsal root entry zones (Figure 2A) and monitored the Ca^{2+} transient amplitude in DRG terminals coming from L4 root fiber tracts, likely C fiber bundles,[43] in response to increasing stimulation intensity (Figure 2B). We recorded the amplitude of Ca^{2+} transients in DRG terminals of the superficial LI in response to a sustained stimulus (Figure 2C). In the sham condition, the minimum stimulus current required to elicit a detectable response was 0.3 mA (Figure 2D). The amplitude of the Ca^{2+} transient increased gradually with the intensity of the stimulus to reach a plateau at 5 mA. In the SNI condition, the stimulus intensity response curve was slightly left-shifted (Figure 2D) with the amplitude of the Ca^{2+} transients significantly increased 3.5- and 2.3-fold for 1 and 2 mA stimuli, respectively, compared with the sham group (Figure 2E). Among the Trpv1$^+$ DRG terminals responding to stimulation, two populations could be identified: one population of terminals was activated with relatively low stimulus intensity with a half-activation of 0.51 ± 0.05 mA (n = 9) and a second population was activated with higher stimulus intensity with a half-activation of 1.92 ± 0.21 mA, n = 9 (Figure 2F). Strikingly, in the SNI group, the low threshold activated population exhibited an even lower half-activation threshold compared with the one for sham animals (0.37 ± 0.02 mA, n = 11, p = 0.01). We also tested whether a frequency dependent effect could be detected on Ca^{2+} transients between the sham and SNI groups. We monitored the variation of GCaMP6s fluorescence in DRG terminals in response to increasing stimulation frequency (from 0.1 to 10 Hz; Figures 2G and 2H). No difference between sham and SNI groups was observed (Figure 2H). Altogether, our data indicate a nerve injury-induced increased of Trpv1$^+$ DRG central terminal excitability.

SNI increases Ca^{2+} transient amplitude in Trpv1$^+$ L4 DRG neuron central terminals in superficial layers in response to a single pulse stimulation

Nociceptors form synapses with second order neurons in the superficial layers of the dorsal horn: with projection neurons in LI, and interneurons in LI and lamina II (LII).[44] We imaged nerve terminals located between 10 and 15 μm from the pia and between 15 and 40 μm from the pia. According to our immunohistochemistry staining (Figure 1F), these layers are CGRP positive (LI and LIIo) and IB4 positive (lamina II inner and LIIo).[41] We assessed the effect of nerve injury on Ca^{2+} transient amplitude in LI (Figures 3A–3D) and in LIIo (Figures 3E–3H). In LI, Trpv1$^+$ DRG terminals appeared like fibers (Figure 3A), whereas in LIIo, Trpv1$^+$ DRG terminals appeared as bouton structures (Figure 3E). The L4 dorsal root was stimulated with a single pulse with increasing intensity and we recorded the variations of GCaMP6s fluorescence (Figures 3B and 3F). The half-activation intensities, similar in both layers (~3 mA), were not modified by the SNI treatment (Figures 3D and 3H). However, we found that in both layers the amplitude of Ca^{2+} transients was increased in the SNI group compared with the sham group (Figures 3C and 3G). Indeed, the signal was potentiated 4.3-fold in LI (from 0.7 ± 0.1 to 3.1 ± 0.5 for sham and SNI, respectively, n = 6, p = 0.0006) and 1.5-fold in LIIo (from 4.5 ± 0.7 to 6.9 ± 0.4 for sham and SNI, respectively, n = 6, p = 0.013). Taken together, these data reveal an increase in excitability of Trpv1$^+$ DRG terminals that spreads to several superficial layers of the dorsal horn.

N- and P/Q-type Ca^{2+} channels contribute to SNI-induced increase in Ca^{2+} transient amplitude in Trpv1$^+$ L4 DRG neuron central terminals

Ca_V channels are the main contributors to Ca^{2+} influx in DRG neurons.[45,46] To determine the contributions of these channels in Trpv1$^+$ neuron terminals, we used a pharmacological approach in which we applied maximal doses of Ca^{2+} channel blockers[12,47–51]: first, we applied the specific N-type Ca^{2+} channel blocker, ω-conotoxin GVIA (GVIA), and then we added the specific P/Q-type Ca^{2+} channel blocker, ω-agatoxin IVA (Aga), with the N-type blocker still present. Preliminary experiments performed on intact spinal cord failed to show any effect of GVIA (1 μM) on Ca^{2+} transients elicited by stimulating the L4 dorsal root with 10 pulses. This concentration of GVIA is typically very effective in blocking N-type currents.[52] Applications of $CdCl_2$ (100 μM) or TTX (1 μM) almost completely abolished Ca^{2+} transients indicating that they relied on the activation of Ca_V channels and on neuronal activity (data not shown). The lack of effect of GVIA on Ca^{2+} transients in the intact spinal cord could possibly be attributed to a poor penetration of the blocker. GVIA is a large peptide (3 kDa) and to facilitate its access to the DRG neuron terminals in the dorsal horn, we incised the spinal cord along the midline beside the imaging area. In these conditions, we obtained between

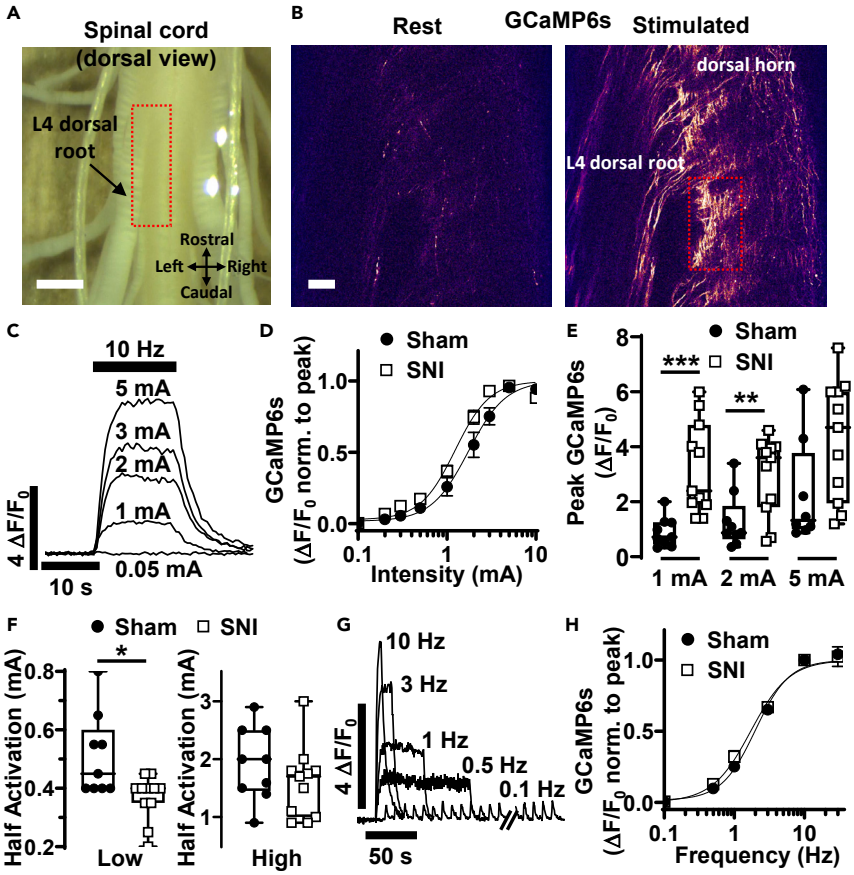

Figure 2. Increase Ca^{2+} transient amplitude in $Trpv1^{+}$ L4 DRG neuron central terminals after SNI in response to a sustained stimulation

(A) The lumbar spinal cord of a Trpv1-CrexAi96 mouse is held dorsal face up in the imaging chamber by a harp and the left L4 dorsal root is placed in a suction electrode to allow electrical stimulation. The dotted red rectangle surrounds the area of the left dorsal horn imaged. Scale bar: 1 mm.

(B) Images of GCaMP6s fluorescence from DRG neuron central terminals in the LI dorsal horn of a Trpv1-CrexAi96 mouse at rest (left panel) and during a stimulation applied to L4 dorsal root (right panel, 5 mA −10 Hz). The dotted red rectangle surrounds the area analyzed. Scale bar: 50 μm.

(C) Traces of GCaMP6s fluorescence from DRG neuron central terminals in response to stimulation applied to L4 dorsal root with increasing intensity (10 Hz stimulation for 15 s from 0.05 mA to 5 mA).

(D) Stimulus intensity-response (GCaMP6s ΔF/F0) plots recorded from DRG neuron central terminals for sham (black dot) and SNI (open square) animals. Responses were normalized to the peak value for 5 mA stimulation for each group. n = 3 to 6 for each point.

(E) Plots showing the average peak GCaMP6s response to 1 mA, 2 mA, and 5 mA stimuli for sham (black dots) and SNI (open circles) groups. 10 ROIs were averaged for each animal. For 1mA, sham = 0.89 ± 0.18, n = 9; SNI = 3.21 ± 0.51, n = 11, ***$p < 0.001$; for 2 mA, sham = 1.28 ± 0.33, n = 9; SNI = 2.96 ± 0.43, n = 11, **$p < 0.01$. For 5 mA, sham = 2.27 ± 0.68, n = 8; SNI = 4.27 ± 0.66, n = 11 (p = 0.054).

(F) Average half-activation intensity for low threshold (low, left panel) and high threshold responding DRG neurons (high, right panel). For low threshold population, the half-activation intensity was 0.51 ± 0.05 mA (n = 9) for the sham and 0.37 ± 0.02 mA (n = 11) for SNI (*p = 0.0102). For the high threshold population, the half-activation intensity was 1.92 ± 0.21 mA (n = 9) for sham and 1.59 ± 0.19 mA (n = 11) for SNI (p = 0.25).

(G) Traces of GCaMP6s fluorescence from DRG neuron processes in response to stimulation applied to L4 dorsal root with increasing frequency (50 pulses between 0.1 and 10 Hz, 2mA).

(H) Plots showing the average peak GCaMP6s response to increasing frequency of stimulation for sham (black dots) and SNI (open circles) groups. n = 4 to 5 for each point. All error bars reflect S.E.M.

36 and 50% inhibition of the Ca^{2+} transients in LI and LIIo with GVIA, and a further 15% inhibition with Aga (200 nM) when the L4 root was stimulated with a single pulse (Figures 4A, 4C, and 4E). Together GVIA and Aga blocked about 70% of the total Ca^{2+} transient. The remaining Ca^{2+} transient is usually attributed to R-, L- and T-type Ca^{2+} channels.[46,53] SNI did not alter the contribution of N and P/Q-type channels to the Ca^{2+} transients. Interestingly, when the L4 root was stimulated with 10 pulses, the N-type contribution to Ca^{2+} transients was estimated at 27.7 ± 3.7% (n = 5) in LIIo and this contribution was significantly reduced to 13.9 ± 2.7% (n = 5, p = 0.016) in the SNI group (Figures 4B, 4D and 4F). This result reveals that, for sustained stimuli, an additional source contributes to the increase of Ca^{2+} transient amplitude observed in LIIo in a chronic pain context. This mechanism is voltage-dependent, but independent of N- and P/Q-type channels and may thus involve contributions from other types of Ca_V or an electrogenic ion exchanger like the Na-Ca exchanger. This possibility will need to be further

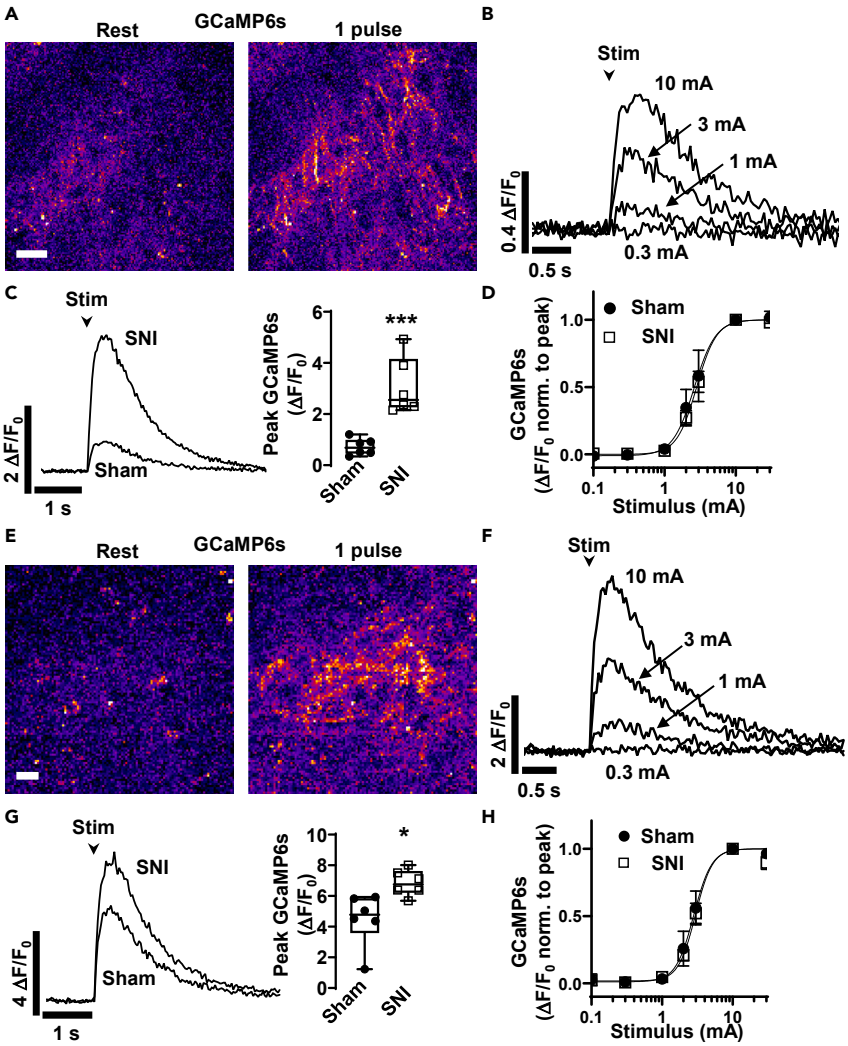

Figure 3. SNI treatment increases single-pulse-induced Ca^{2+} transient amplitude in $Trpv1^{+}$ L4 DRG neuron central terminals in superficial layers of the spinal dorsal horn

(A) GCaMP6s fluorescence from DRG neuron central terminals in the lamina I dorsal horn of a Trpv1-CrexAi96 mouse at rest (left) and during a single-pulse stimulation (1 pulse, right) applied to L4 dorsal root (10 mA). Scale bar: 20 μm.

(B) Traces of GCaMP6s fluorescence from DRG neuron central terminals in the lamina I dorsal horn in response to a single-pulse stimulation applied to L4 dorsal root with increasing intensity (from 0.3 mA to 10 mA).

(C) Average traces of GCaMP6s fluorescence from DRG neuron central terminals in the lamina I dorsal horn of sham and SNI Trpv1-CrexAi96 mice in response to a single-pulse stimulation (10 mA) applied to L4 dorsal root. Plots showing the average peak GCaMP6s response to a 10 mA single-pulse stimulation for sham (black dots) and SNI (open circles) groups. n = 6 animals. 10 ROIs were averaged for each animal. ***p = 0.006.

(D) Stimulus intensity-response (GCaMP6s ΔF/F0) plots recorded from DRG neuron central terminals in the lamina I dorsal horn of sham (black dots) and SNI (open circles) Trpv1-CrexAi96 mice. Responses were normalized to the peak value for 10 mA stimulation for each group. n = 3 to 6 for each point. EC 50 = 2.6 mA and 2.8 mA for sham and SNI, respectively.

(E) GCaMP6s fluorescence from DRG neuron central terminals in the lamina II outer dorsal horn of a Trpv1-CrexAi96 mouse at rest (left) and during a single-pulse stimulation (1 pulse, right) applied to L4 dorsal root (10 mA). Scale bar: 10 μm.

(F) Traces of GCaMP6s fluorescence from DRG neuron central terminals in the lamina II outer in response to a single-pulse stimulation applied to L4 dorsal root with increasing intensity (from 0.3 mA to 10 mA).

(G) Average traces of GCaMP6s fluorescence from DRG neuron central terminals in the lamina II outer dorsal horn of sham and SNI Trpv1-CrexAi96 mice in response to a single-pulse stimulation (10 mA) applied to L4 dorsal root. Plots showing the average peak GCaMP6s response to a 10 mA single-pulse stimulation for sham (black dots) and SNI (open circles) groups. n = 6 animals. 10 ROIs were averaged for each animal. *p = 0.013.

(H) Stimulus intensity-response (GCaMP6s ΔF/F0) plots recorded from DRG neuron central terminals in the lamina II outer for sham (black dot) and SNI (open square) animals. Responses were normalized to the peak value for 10 mA stimulation for each group. n = 3 to 6 for each point. EC 50 = 2.8 mA and 3.0 mA for sham and SNI, respectively. All error bars reflect S.E.M.

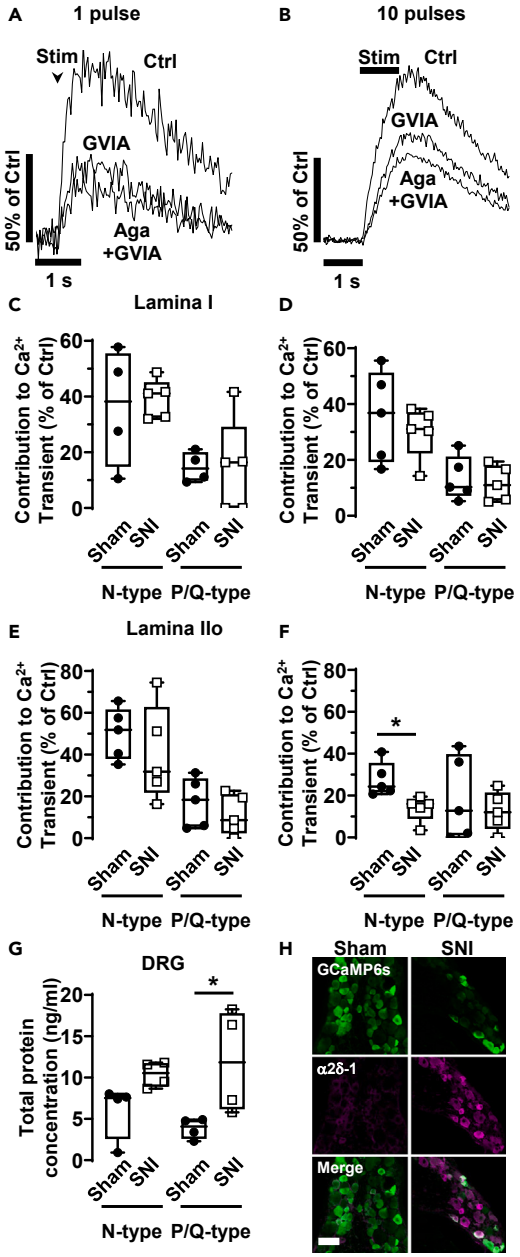

Figure 4. N- and P/Q-type Ca^{2+} channel contributions to Ca^{2+} transients in $Trpv1^+$ L4 DRG neuron central terminals in superficial layers of the spinal dorsal horn

(A and B) GCaMP6s fluorescence variations from $Trpv1^+$ DRG neuron central terminals in superficial layers of the spinal dorsal horn in response to 1 pulse (A) and 10 pulses (B) at 3 mA before (Ctrl), 20 min after application of ω-conotoxin GVIA (GVIA, 1 μM) and 20 min after adding ω-agatoxin IVA (Aga, 200 nM, Aga+GVIA) to GVIA.

(C–F) Average contributions of N- and P/Q-type channels to Ca^{2+} transients in response to 1 pulse (C and E) and 10 pulses (D and F) in $Trpv1^+$ DRG terminals in lamina I (C and D) and in lamina IIo (E and F). (C) Contribution of VGCCs in response to 1 pulse in lamina I: N-type, sham = 36.2 ± 10.6% (n = 4) and SNI = 39.2 ± 3.1% (n = 5), p = 0.77; P/Q-type: sham = 14.7 ± 2.7% (n = 4); SNI = 14.9 ± 7.6% (n = 5), p = 0.98. (D) Contribution of VGCCs in response to 10 pulses in lamina I: N-type, sham = 35.6 ± 7.3% (n = 5) and SNI = 30.0 ± 4.2% (n = 5), p = 0.53; P/Q-type, sham = 13.4 ± 3.5% (n = 5) and SNI = 11.6 ± 2.9% (n = 5), p = 0.70. (E) Contribution of VGCCs in response to 1 pulse in lamina IIo: N-type, sham = 50.2 ± 5.5% (n = 5) and SNI = 40.2 ± 10.3% (n = 5), p = 0.42; P/Q-type, sham = 17.3 ± 5.3% (n = 5) and SNI = 11.1 ± 4.3% (n = 5), p = 0.39. (F) Contribution of VGCCs in response to 10 pulses in lamina IIo: N-type, sham = 27.7 ± 3.7% (n = 5) and SNI = 13.9 ± 2.7% (n = 5), *p = 0.0164; P/Q-type, sham = 18.9 ± 8.09 (n = 5) and SNI = 12.6 ± 4.2% (n = 5), p = 0.54.

(G) Variations of N- and P/Q-type Ca^{2+} channel protein expression in ipsilateral L4 DRG following SNI treatment. ELISA techniques were used to quantify total channel protein concentration from DRG. Proteins were extracted from individual ipsilateral L4 DRGs (5 DRGs for each condition). Because of low extraction yield, 2 samples had to be pooled to obtain enough total protein to reliably run the ELISA. N-type total protein: sham = 5.99 ± 1.7 ng/mL; SNI = 10.4 ± 0.8 ng/mL (p = 0.055, n = 4). P/Q-type total protein: sham = 3.8 ± 0.6 ng/mL and SNI = 11.9 ± 3.2 ng/mL (p = 0.045, n = 4). *p < 0.05.

(H) Confocal images of GCaMP6s and $Ca_V\alpha2$-δ-1 expression in ipsilateral L4 DRG of a Trpv1-Cre x Ai96 mouse. DRG sections were immunostained with GFP Ab (stains GCaMP6s—green) and $Ca_V\alpha2$-δ-1 Ab (α2-δ-1—magenta). The merged image shows the increase of $Ca_V\alpha2$-δ-1 expression in GCaMP6s positive DRG neurons (bottom panel). The intensity of $Ca_V\alpha2$-δ-1 staining was quantified from GCaMP6s positive neurons: sham = 7.3 ± 0.2 a.u. (n = 186 neurons) vs. SNI 15.5 ± 0.4 a.u. (n = 342 neurons, p < 0.0001) (7 and 14 sections were imaged from sham and SNI group, respectively—2 animals per group). Scale bar: 50 μm. All error bars reflect S.E.M.

explored. Altogether, these data show that the SNI-induced increase of Ca^{2+} transient amplitude involves N- and P/Q-type channels and an additional, still unknown, mechanism.

An increase in functional $Ca_V2.X$ channels at presynaptic terminals of DRG neurons could be due to an increase in total protein and/or an increase in the trafficking of the channels. To try to tease out the mechanism(s) involved, we quantified the total expression of N- and P/Q-type channels in ipsilateral L4 DRG. Using an ELISA method, we showed that following SNI treatment the N-type channel protein levels increased by 1.7-fold compared with the sham group (Figure 4G) although this effect just missed statistical significance (n = 4, p = 0.055). Moreover, the expression of P/Q type channels was significantly increased by more than 3-fold in SNI-treated ipsilateral L4 ganglia compared with sham condition (n = 4, p = 0.045; Figure 4G). The auxiliary $Ca_V\alpha2$-δ1 subunit is key for trafficking of $Ca_V2.X$ channels to synaptic sites[54] and it was shown to be increased in chronic pain models.[9,10,55] Using immunohistochemistry staining, we showed that the expression of $Ca_V\alpha2$-δ1 was upregulated by about 2-fold in GCaMP6 positive DRG neuron somata following SNI treatment (Figure 4H). Altogether, the upregulation of both $Ca_V2.X$ total protein and $Ca_V\alpha2$-δ1 subunit can contribute to the increase of functional N- and P/Q-type channels at the central terminals of DRG neurons.

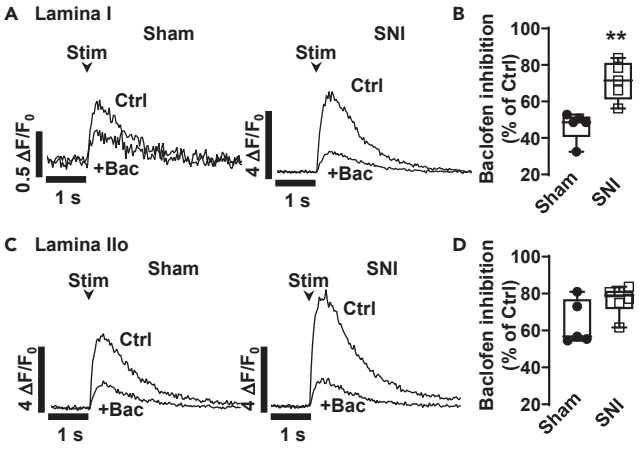

Figure 5. GABA-B-dependent inhibition on Ca^{2+} transient amplitude is increased in $Trpv1^+$ L4 DRG neuron central terminals in the laminae of the dorsal horn I during chronic pain

(A) Average traces of GCaMP6s fluorescence from DRG neuron central terminals in the lamina I dorsal horn of sham (left panel) and SNI (right panel) Trpv1-CrexAi96 mice in response to a single-pulse stimulation (10 mA) applied to L4 dorsal root before (Ctrl) and after baclofen application (+Bac, 100 μM).

(B) Plot showing the magnitude of the inhibition of baclofen (100 μM) on the Ca^{2+} transient recorded from DRG neuron central terminals in the lamina I dorsal horn of sham and SNI Trpv1-CrexAi96 mice in response to a single-pulse stimulation (10 mA). Sham = 46.6 ± 3.6% (n = 5) and SNI = 71.2 ± 4.8% (n = 5); **p = 0.0036.

(C) Average traces of GCaMP6s fluorescence from DRG neuron central terminals in the lamina II outer dorsal horn of sham (left) and SNI (right) Trpv1-CrexAi96 mice in response to a single-pulse stimulation (10 mA) applied to L4 dorsal root before (Ctrl) and after baclofen application (+Bac, 100 μM).

(D) Plot showing the magnitude of the inhibition of baclofen (100 μM) on the Ca^{2+} transient recorded from DRG neuron central terminals in the lamina II outer dorsal horn of sham and SNI Trpv1crexAi96 mice in response to a single-pulse stimulation (10 mA). Sham = 64.1 ± 5.4% (n = 5) and SNI = 76.5 ± 3.2% (n = 6), p = 0.0714. All error bars reflect S.E.M.

Increased GABA-B receptor-dependent inhibition of Ca^{2+} transients in $Trpv1^+$ DRG terminals in LI

GABA-B receptors are potent modulators of $Ca_V2.X$ channels[1] and gamma-aminobutyric acid (GABA) modulation is known to be altered during chronic pain.[56] We tested the effect of baclofen, a GABA-B receptor agonist, on the amplitude of Ca^{2+} transients in response to a single-pulse stimulation of the L4 dorsal root (Figure 5). In the sham group, baclofen inhibited 46.6 ± 3.6% (n = 5) and 64.1 ± 5.4% (n = 5) of the Ca^{2+} transients in LI and LIIo, respectively (Figures 5B and 5D). After SNI, the effect of baclofen was not modified in LIIo (76.5 ± 3.2%, n = 6, p = 0.0714). However, in LI, baclofen-dependent inhibition was increased to 71.2 ± 4.8% (n = 5, p = 0.0036). These data demonstrate that GABA-B receptor mediated inhibition of Ca_V channels is upregulated in $Trpv1^+$ DRG terminals during neuropathic pain states.

DISCUSSION

Our findings show an increase of Ca^{2+} transient amplitude in the central terminals of $Trpv1^+$ DRG neurons in chronic pain conditions. We also show that both N- and P/Q-type channels contribute critically to this increase in Ca^{2+} transient amplitude. Finally, we show that GABA-B receptor inhibitory control on Ca^{2+} transient is potentiated in the superficial lamina of the dorsal horn following chronic pain.

In numerous chronic pain models increases in $Ca_V2.2$ protein expression in DRG neuron somata and in dorsal horn superficial layers have been reported,[21–26,57] but increases in dorsal horn $Ca_V2.2$ levels could not be attributed clearly to nerve terminals of afferent fibers. On the other hand, in a recent study performed in a mouse model of partial sciatic nerve ligation, $Ca_V2.2$ immunostaining was shown to decrease in patches in the superficial layers of the dorsal horn.[25] This decrease of $Ca_V2.2$ immunostaining co-occurred with a decrease of staining for presynaptic markers CGRP and IB4 suggesting a loss of sensory terminals due to the partial ligation of the sciatic nerve. Further investigations will be needed in this latter model to examine whether the remaining primary afferent terminals exhibit an alteration of Ca^{2+} transient amplitude in the superficial layers of the dorsal horn.

Although $Ca_V2.X$ channels are key to synaptic transmission between primary afferent neurons and spinal neurons, functional data focusing on presynaptic $Ca_V2.X$ channels have been scarce and typically based on spinal cord slice recordings in which it has been difficult to discriminate synaptic inputs from afferent fibers and interneurons[3,27,29,58] (but see study by Stemkowski et al.[28]). Two reports have revealed an alteration in voltage-gated Ca^{2+} channel mediated postsynaptic responses in spinal cord slices.[26,59] However, amplitudes of postsynaptic responses do not depend linearly on the magnitude of presynaptic calcium influx. To date, similar results had not been reported in *ex vivo* preparations that preserve the architecture of the spinal cord and the connections with dorsal roots, and to our knowledge, no direct investigation of the effects of nerve injury on presynaptic calcium levels had been reported. We provide here evidence that N- and P/Q-type calcium channels are functionally dysregulated in sensory neuron nerve terminals in both LI and LII of the intact spinal cord in response to a peripheral nerve injury. By using Cre-dependent expression of a Ca^{2+} indicator, we were able to attribute Ca^{2+} channel activity directly to afferent fiber terminals, with no contamination from interneurons.

$Ca_V2.1$ channels are not considered appropriate pharmacological targets for pain compared with $Ca_V2.2$ channels.[1] However, we show here that the contribution of $Ca_V2.1$ channels to the increased Ca^{2+} transient is far from negligible and strategies targeting both $Ca_V2.2$ and $Ca_V2.1$ could be promising avenues to treat chronic pain. In this context, a recent study from the Colecraft lab has revealed that by modulating the degradation rate of auxiliary Cavβ subunits, which are critical for the plasma membrane trafficking of both $Ca_V2.1$ and $Ca_V2.2$ channels, they could successfully control the expression of Ca_V channels in DRG neurons and attenuate the development of allodynia in a mouse model of chronic pain.[60]

In normal physiological conditions, nociceptors are under strong presynaptic GABAergic regulation and our observations in sham operated animals corroborate this statement (Figure 5).[61] In chronic pain models, a loss of inhibition mediated by GABA has been observed in both pre- and postsynaptic compartments.[56] We show that, in LI only, baclofen inhibition of Ca_V channel mediated-Ca^{2+} signals is potentiated after SNI which may suggest a tighter modulation of Ca_V channels by GABA-B receptors. It is possible that this increase of GABA-B receptor inhibition constitutes a compensatory mechanism to counteract the increase in excitability of $Trpv1^+$ nociceptors but further investigations are warranted to demonstrate this point. We note, however, that there is not a linear relationship between Ca^{2+} levels measured by Ca^{2+} imaging and Ca^{2+} flux via whole-cell currents. It is thus possible that the increased baclofen effect may reflect the fact that Ca^{2+} channel activity is potently upregulated in SNI conditions in LI and much more so than in LII. We expect that the majority of the baclofen effect on Ca^{2+} levels is mediated by an action on $Ca_V2.2$, as these channels are more potently inhibited by G proteins than $Ca_V2.1$[62] and contribute more strongly to the observed Ca^{2+} transients.

The use of a sustained stimulation protocol allowed us to unmask two populations of $Trpv1^+$ DRG neurons that differ in their activation threshold. Recent single cell RNA-sequencing studies have categorized ~19 molecular types of DRG sensory neurons in adult mouse including five types expressing Trpv1 channel transcript.[63–67] Among these five $Trpv1^+$ types of DRG neurons, four were classified as C-type (C-nociceptor C-mechano heat types) and one as Aδ-type (Aδ heat-nociceptor type). Aδ-type DRG neurons are activated by lower intensity stimulus than C-type DRG neurons.[68] We can then assume that the two $Trpv1^+$ DRG neuron populations that we detected correspond to one population of Aδ-type neurons and, at least, one population of C-type neurons. Also, the excitability of Aδ-type neurons has been shown to be increased in a chronic pain context[69] which is consistent with the decrease of activation threshold we observed for the low threshold activated population of $Trpv1^+$ DRG neurons following the SNI treatment.

Ca^{2+} transients recorded in response to a single pulse stimulation reflect mainly the activity of Ca_V channels whereas Ca^{2+} transients recorded in response to a sustain stimulus sums the activity of Ca_V channels and additional Ca^{2+} regulatory mechanisms such as the of Na^+/Ca^{2+} exchanger, Ca^{2+} ATPases, mitochondria and Ca^{2+}-induce Ca^{2+} release from the endoplasmic reticulum.[70] Interestingly, the activation threshold of the low threshold $Trpv1^+$ DRG neurons by a sustain stimulus is decreased following SNI treatment which suggests that Ca^{2+} regulatory mechanisms contribute to this effect. The precise nature of the Ca^{2+} regulatory mechanisms involved in this pain model is yet to be identified although some of these mechanisms have been shown to be affected in chronic pain context.[71–75]

Here, we took advantage of 2-photon microscopy to image the intact spinal cord and monitor the functional remodeling of Ca_V channels in the presynaptic terminals of DRG neurons in the superficial layers of the dorsal horn following nerve injury that gives rise to neuropathic pain. Our study focused on a subset of primary sensory neurons expressing Trpv1; however, a similar strategy could be applied to investigate other populations of DRG neurons.[76] Also, the highly versatile properties of adeno-associated viruses provide the opportunity to target the expression of various genetically encoded fluorescent reporter genes, including that of glutamate release (iGluSnFR), to DRG neurons.[77,78] Our study then lays the foundation for future experiments that should focus on physiological consequences of the remodeling of presynaptic Ca_V channels on neurotransmitter release.

Limitations of the study

We consider two potential limitations of our study. First, as outlined previously, expression of our calcium indicator in Trpv1-Cre mice does not imply that all of the neurons that express GCaMP6s do in fact coexpress Trpv1 channels, and thus are likely a combination of C and A fibers. This does not affect our conclusion that calcium channels are dysregulated in afferent fiber terminals after peripheral nerve injury. Second, we applied N-type and P/Q-type channel blockers sequentially in that order. Given that intracellular calcium concentration does not depend linearly on calcium entry via particular class of calcium channels, it is possible that reversing the order of application may uncover a different relative contribution of N-type and P/Q-type channels. That said, because the same paradigm was applies in all experiments, the conclusion that SNI affects N-type and P/Q-type levels holds.

STAR★METHODS

Detailed methods are provided in the online version of this paper and include the following:

- KEY RESOURCES TABLE
- RESOURCE AVAILABILITY
  - Lead contact
  - Materials availability
  - Data and code availability
- EXPERIMENTAL MODEL AND STUDY PARTICIPANT DETAILS
  - Mouse breeding

ACKNOWLEDGMENTS

This work was supported by grants to G.W.Z. and P.K.S. from the Canadian Institutes of Health Research (CIHR) and Infrastructure funded by the Canada Foundation for Innovation. E.K.H. is funded by a CIHR Fellowship. We thank Lina Chen for technical assistance and Dr. Zizhen Zhang for his expertise on spared nerve injury surgery.

DECLARATION OF INTERESTS

The authors declare no competing interests.

Received: January 29, 2024
Revised: April 29, 2024
Accepted: May 10, 2024
Published: May 14, 2024

REFERENCES

1. Zamponi, G.W., Striessnig, J., Koschak, A., and Dolphin, A.C. (2015). The Physiology, Pathology, and Pharmacology of Voltage-Gated Calcium Channels and Their Future Therapeutic Potential. Pharmacol. Rev. *67*, 821–870. https://doi.org/10.1124/pr.114.009654.
2. Dolphin, A.C., and Lee, A. (2020). Presynaptic calcium channels: specialized control of synaptic neurotransmitter release. Nat. Rev. Neurosci. *21*, 213–229. https://doi.org/10.1038/s41583-020-0278-2.
3. Heinke, B., Balzer, E., and Sandkühler, J. (2004). Pre- and postsynaptic contributions of voltage-dependent Ca2+ channels to nociceptive transmission in rat spinal lamina I neurons. Eur. J. Neurosci. *19*, 103–111. https://doi.org/10.1046/j.1460-9568.2003.03083.x.
4. Ferron, L., Koshti, S., and Zamponi, G.W. (2021). The life cycle of voltage-gated Ca^{2+} channels in neurons: an update on the trafficking of neuronal calcium channels. Neuronal Signal. *5*, NS20200095. https://doi.org/10.1042/NS20200095.
5. Geisler, S., Schöpf, C.L., and Obermair, G.J. (2015). Emerging evidence for specific neuronal functions of auxiliary calcium channel αεδ subunits. Gen. Physiol. Biophys. *34*, 105–118. https://doi.org/10.4149/gpb_2014037.
6. Dolphin, A.C. (2012). Calcium channel auxiliary α2δ and β subunits: trafficking and one step beyond. Nat. Rev. Neurosci. *13*, 542–555. https://doi.org/10.1038/nrn3311.
7. Zamponi, G.W. (2016). Targeting voltage-gated calcium channels in neurological and psychiatric diseases. Nat. Rev. Drug Discov. *15*, 19–34. https://doi.org/10.1038/nrd.2015.5.
8. Patel, R., Montagut-Bordas, C., and Dickenson, A.H. (2018). Calcium channel modulation as a target in chronic pain control. Br. J. Pharmacol. *175*, 2173–2184. https://doi.org/10.1111/bph.13789.
9. Bauer, C.S., Nieto-Rostro, M., Rahman, W., Tran-Van-Minh, A., Ferron, L., Douglas, L., Kadurin, I., Sri Ranjan, Y., Fernandez-Alacid, L., Millar, N.S., et al. (2009). The increased trafficking of the calcium channel subunit alpha2delta-1 to presynaptic terminals in neuropathic pain is inhibited by the alpha2delta ligand pregabalin. J. Neurosci. *29*, 4076–4088. https://doi.org/10.1523/JNEUROSCI.0356-09.2009.
10. Luo, Z.D., Calcutt, N.A., Higuera, E.S., Valder, C.R., Song, Y.H., Svensson, C.I., and Myers, R.R. (2002). Injury type-specific calcium channel alpha 2 delta-1 subunit up-regulation in rat neuropathic pain models correlates with antiallodynic effects of gabapentin. J. Pharmacol. Exp. Ther. *303*, 1199–1205. https://doi.org/10.1124/jpet.102.041574.
11. Newton, R.A., Bingham, S., Case, P.C., Sanger, G.J., and Lawson, S.N. (2001). Dorsal root ganglion neurons show increased expression of the calcium channel alpha2delta-1 subunit following partial sciatic nerve injury. Brain Res. Mol. Brain Res. *95*, 1–8. https://doi.org/10.1016/s0169-328x(01)00188-7.
12. Cassidy, J.S., Ferron, L., Kadurin, I., Pratt, W.S., and Dolphin, A.C. (2014). Functional exofacially tagged N-type calcium channels elucidate the interaction with auxiliary α2δ-1 subunits. Proc. Natl. Acad. Sci. USA *111*, 8979–8984. https://doi.org/10.1073/pnas.1403731111.
13. Field, M.J., Cox, P.J., Stott, E., Melrose, H., Offord, J., Su, T.Z., Bramwell, S., Corradini, L., England, S., Winks, J., et al. (2006). Identification of the alpha2-delta-1 subunit of voltage-dependent calcium channels as a molecular target for pain mediating the analgesic actions of pregabalin. Proc. Natl. Acad. Sci. USA *103*, 17537–17542. https://doi.org/10.1073/pnas.0409066103.
14. Kricek, F., Ruf, C., Meghani, P., Souza, I.A., Gandini, M.A., Zamponi, G.W., and Skouteris, G. (2024). A next generation peripherally restricted Cavα2δ-1 ligand with inhibitory action on Cav2.2 channels and utility in neuropathic pain. Biomed. Pharmacother. *174*, 116472. https://doi.org/10.1016/j.biopha.2024.116472.
15. Staats, P.S., Yearwood, T., Charapata, S.G., Presley, R.W., Wallace, M.S., Byas-Smith, M., Fisher, R., Bryce, D.A., Mangieri, E.A., Luther, R.R., et al. (2004). Intrathecal ziconotide in the treatment of refractory pain in patients with cancer or AIDS: a randomized controlled trial. JAMA *291*, 63–70. https://doi.org/10.1001/jama.291.1.63.
16. Miljanich, G.P. (2004). Ziconotide: neuronal calcium channel blocker for treating severe chronic pain. Curr. Med. Chem. *11*, 3029–3040. https://doi.org/10.2174/0929867043363884.
17. Costigan, M., Scholz, J., and Woolf, C.J. (2009). Neuropathic pain: a maladaptive response of the nervous system to damage. Annu. Rev. Neurosci. *32*, 1–32. https://doi.org/10.1146/annurev.neuro.051508.135531.
18. von Hehn, C.A., Baron, R., and Woolf, C.J. (2012). Deconstructing the neuropathic pain phenotype to reveal neural mechanisms. Neuron *73*, 638–652. https://doi.org/10.1016/j.neuron.2012.02.008.
19. Bourinet, E., Altier, C., Hildebrand, M.E., Trang, T., Salter, M.W., and Zamponi, G.W. (2014). Calcium-permeable ion channels in pain signaling. Physiol. Rev. *94*, 81–140. https://doi.org/10.1152/physrev.00023.2013.
20. Waxman, S.G., and Zamponi, G.W. (2014). Regulating excitability of peripheral afferents: emerging ion channel targets. Nat. Neurosci. *17*, 153–163. https://doi.org/10.1038/nn.3602.
21. Cizkova, D., Marsala, J., Lukacova, N., Marsala, M., Jergova, S., Orendacova, J., and Yaksh, T.L. (2002). Localization of N-type Ca2+ channels in the rat spinal cord following chronic constrictive nerve injury. Exp. Brain Res. *147*, 456–463. https://doi.org/10.1007/s00221-002-1217-3.
22. Yokoyama, K., Kurihara, T., Makita, K., and Tanabe, T. (2003). Plastic change of N-type Ca channel expression after preconditioning is responsible for prostaglandin E2-induced long-lasting allodynia. Anesthesiology *99*, 1364–1370. https://doi.org/10.1097/00000542-200312000-00019.

23. Umeda, M., Ohkubo, T., Ono, J., Fukuizumi, T., and Kitamura, K. (2006). Molecular and immunohistochemical studies in expression of voltage-dependent Ca2+ channels in dorsal root ganglia from streptozotocin-induced diabetic mice. Life Sci. *79*, 1995–2000. https://doi.org/10.1016/j.lfs.2006.06.039.
24. Altier, C., Dale, C.S., Kisilevsky, A.E., Chapman, K., Castiglioni, A.J., Matthews, E.A., Evans, R.M., Dickenson, A.H., Lipscombe, D., Vergnolle, N., and Zamponi, G.W. (2007). Differential role of N-type calcium channel splice isoforms in pain. J. Neurosci. *27*, 6363–6373. https://doi.org/10.1523/JNEUROSCI.0307-07.2007.
25. Nieto-Rostro, M., Patel, R., Dickenson, A.H., and Dolphin, A.C. (2023). Nerve injury increases native Ca V 2.2 trafficking in dorsal root ganglion mechanoreceptors. Pain *164*, 1264–1279. https://doi.org/10.1097/j.pain.0000000000002846.
26. Takasu, K., Ogawa, K., Minami, K., Shinohara, S., and Kato, A. (2016). Injury-specific functional alteration of N-type voltage-gated calcium channels in synaptic transmission of primary afferent C-fibers in the rat spinal superficial dorsal horn. Eur. J. Pharmacol. *772*, 11–21. https://doi.org/10.1016/j.ejphar.2015.12.031.
27. García-Caballero, A., Gadotti, V.M., Stemkowski, P., Weiss, N., Souza, I.A., Hodgkinson, V., Bladen, C., Chen, L., Hamid, J., Pizzoccaro, A., et al. (2014). The deubiquitinating enzyme USP5 modulates neuropathic and inflammatory pain by enhancing Cav3.2 channel activity. Neuron *83*, 1144–1158. https://doi.org/10.1016/j.neuron.2014.07.036.
28. Stemkowski, P., García-Caballero, A., Gadotti, V.D.M., M'Dahoma, S., Huang, S., Black, S.A.G., Chen, L., Souza, I.A., Zhang, Z., and Zamponi, G.W. (2016). TRPV1 Nociceptor Activity Initiates USP5/T-type Channel-Mediated Plasticity. Cell Rep. *17*, 2901–2912. https://doi.org/10.1016/j.celrep.2016.11.047.
29. Jacus, M.O., Uebele, V.N., Renger, J.J., and Todorovic, S.M. (2012). Presynaptic Cav3.2 channels regulate excitatory neurotransmission in nociceptive dorsal horn neurons. J. Neurosci. *32*, 9374–9382. https://doi.org/10.1523/JNEUROSCI.0068-12.2012.
30. Lu, Y., Doroshenko, M., Lauzadis, J., Kanjiya, M.P., Rebecchi, M.J., Kaczocha, M., and Puopolo, M. (2018). Presynaptic Inhibition of Primary Nociceptive Signals to Dorsal Horn Lamina I Neurons by Dopamine. J. Neurosci. *38*, 8809–8821. https://doi.org/10.1523/JNEUROSCI.0323-18.2018.
31. Yoshimura, M., and Jessell, T. (1990). Amino acid-mediated EPSPs at primary afferent synapses with substantia gelatinosa neurones in the rat spinal cord. J. Physiol. *430*, 315–335. https://doi.org/10.1113/jphysiol.1990.sp018293.
32. Lee, C.J., Bardoni, R., Tong, C.K., Engelman, H.S., Joseph, D.J., Magherini, P.C., and MacDermott, A.B. (2002). Functional expression of AMPA receptors on central terminals of rat dorsal root ganglion neurons and presynaptic inhibition of glutamate release. Neuron *35*, 135–146. https://doi.org/10.1016/s0896-6273(02)00729-8.
33. Harding, E.K., Boivin, B., and Salter, M.W. (2020). Intracellular Calcium Responses Encode Action Potential Firing in Spinal Cord Lamina I Neurons. J. Neurosci. *40*, 4439–4456. https://doi.org/10.1523/JNEUROSCI.0206-20.2020.
34. Wang, F., Bélanger, E., Paquet, M.E., Côté, D.C., and De Koninck, Y. (2016). Probing pain pathways with light. Neuroscience *338*, 248–271. https://doi.org/10.1016/j.neuroscience.2016.09.035.
35. Johannssen, H.C., and Helmchen, F. (2010). In vivo Ca2+ imaging of dorsal horn neuronal populations in mouse spinal cord. J. Physiol. *588*, 3397–3402. https://doi.org/10.1113/jphysiol.2010.191833.
36. Ran, C., Hoon, M.A., and Chen, X. (2016). The coding of cutaneous temperature in the spinal cord. Nat. Neurosci. *19*, 1201–1209. https://doi.org/10.1038/nn.4350.
37. Tang, P., Zhang, Y., Chen, C., Ji, X., Ju, F., Liu, X., Gan, W.B., He, Z., Zhang, S., Li, W., and Zhang, L. (2015). In vivo two-photon imaging of axonal dieback, blood flow, and calcium influx with methylprednisolone therapy after spinal cord injury. Sci. Rep. *5*, 9691. https://doi.org/10.1038/srep09691.
38. Cavanaugh, D.J., Chesler, A.T., Jackson, A.C., Sigal, Y.M., Yamanaka, H., Grant, R., O'Donnell, D., Nicoll, R.A., Shah, N.M., Julius, D., and Basbaum, A.I. (2011). Trpv1 reporter mice reveal highly restricted brain distribution and functional expression in arteriolar smooth muscle cells. J. Neurosci. *31*, 5067–5077. https://doi.org/10.1523/JNEUROSCI.6451-10.2011.
39. Kim, Y.S., Anderson, M., Park, K., Zheng, Q., Agarwal, A., Gong, C., LaVinka, P.C., Saijilafu, H., Young, L., He, S., et al. (2016). Coupled Activation of Primary Sensory Neurons Contributes to Chronic Pain. Neuron *91*, 1085–1096. https://doi.org/10.1016/j.neuron.2016.07.044.
40. Tominaga, M., Caterina, M.J., Malmberg, A.B., Rosen, T.A., Gilbert, H., Skinner, K., Raumann, B.E., Basbaum, A.I., and Julius, D. (1998). The cloned capsaicin receptor integrates multiple pain-producing stimuli. Neuron *21*, 531–543. https://doi.org/10.1016/s0896-6273(00)80564-4.
41. Chen, C.L., Broom, D.C., Liu, Y., de Nooij, J.C., Li, Z., Cen, C., Samad, O.A., Jessell, T.M., Woolf, C.J., and Ma, Q. (2006). Runx1 determines nociceptive sensory neuron phenotype and is required for thermal and neuropathic pain. Neuron *49*, 365–377. https://doi.org/10.1016/j.neuron.2005.10.036.
42. Cavanaugh, D.J., Chesler, A.T., Bráz, J.M., Shah, N.M., Julius, D., and Basbaum, A.I. (2011). Restriction of transient receptor potential vanilloid-1 to the peptidergic subset of primary afferent neurons follows its developmental downregulation in nonpeptidergic neurons. J. Neurosci. *31*, 10119–10127. https://doi.org/10.1523/JNEUROSCI.1299-11.2011.
43. Harty, B.L., and Monk, K.R. (2017). Unwrapping the unappreciated: recent progress in Remak Schwann cell biology. Curr. Opin. Neurobiol. *47*, 131–137. https://doi.org/10.1016/j.conb.2017.10.003.
44. Todd, A.J. (2010). Neuronal circuitry for pain processing in the dorsal horn. Nat. Rev. Neurosci. *11*, 823–836. https://doi.org/10.1038/nrn2947.
45. Ferron, L., Nieto-Rostro, M., Cassidy, J.S., and Dolphin, A.C. (2014). Fragile X mental retardation protein controls synaptic vesicle exocytosis by modulating N-type calcium channel density. Nat. Commun. *5*, 3628. https://doi.org/10.1038/ncomms4628.
46. Ferron, L., Novazzi, C.G., Pilch, K.S., Moreno, C., Ramgoolam, K., and Dolphin, A.C. (2020). FMRP regulates presynaptic localization of neuronal voltage gated calcium channels. Neurobiol. Dis. *138*, 104779. https://doi.org/10.1016/j.nbd.2020.104779.
47. McCleskey, E.W., Fox, A.P., Feldman, D.H., Cruz, L.J., Olivera, B.M., Tsien, R.W., and Yoshikami, D. (1987). Omega-conotoxin: direct and persistent blockade of specific types of calcium channels in neurons but not muscle. Proc. Natl. Acad. Sci. USA *84*, 4327–4331. https://doi.org/10.1073/pnas.84.12.4327.
48. Boland, L.M., Morrill, J.A., and Bean, B.P. (1994). omega-Conotoxin block of N-type calcium channels in frog and rat sympathetic neurons. J. Neurosci. *14*, 5011–5027. https://doi.org/10.1523/JNEUROSCI.14-08-05011.1994.
49. Mintz, I.M., Venema, V.J., Swiderek, K.M., Lee, T.D., Bean, B.P., and Adams, M.E. (1992). P-type calcium channels blocked by the spider toxin omega-Aga-IVA. Nature *355*, 827–829. https://doi.org/10.1038/355827a0.
50. Bourinet, E., Soong, T.W., Sutton, K., Slaymaker, S., Mathews, E., Monteil, A., Zamponi, G.W., Nargeot, J., and Snutch, T.P. (1999). Splicing of alpha 1A subunit gene generates phenotypic variants of P- and Q-type calcium channels. Nat. Neurosci. *2*, 407–415. https://doi.org/10.1038/8070.
51. Brockhaus, J., Brüggen, B., and Missler, M. (2019). Imaging and Analysis of Presynaptic Calcium Influx in Cultured Neurons Using synGCaMP6f. Front. Synaptic Neurosci. *11*, 12. https://doi.org/10.3389/fnsyn.2019.00012.
52. Ellinor, P.T., Zhang, J.F., Horne, W.A., and Tsien, R.W. (1994). Structural determinants of the blockade of N-type calcium channels by a peptide neurotoxin. Nature *372*, 272–275. https://doi.org/10.1038/372272a0.
53. Murali, S.S., Napier, I.A., Mohammadi, S.A., Alewood, P.F., Lewis, R.J., and Christie, M.J. (2015). High-voltage-activated calcium current subtypes in mouse DRG neurons adapt in a subpopulation-specific manner after nerve injury. J. Neurophysiol. *113*, 1511–1519. https://doi.org/10.1152/jn.00608.2014.
54. Hoppa, M.B., Lana, B., Margas, W., Dolphin, A.C., and Ryan, T.A. (2012). $\alpha 2\delta$ expression sets presynaptic calcium channel abundance and release probability. Nature *486*, 122–125. https://doi.org/10.1038/nature11033.
55. Patel, R., Bauer, C.S., Nieto-Rostro, M., Margas, W., Ferron, L., Chaggar, K., Crews, K., Ramirez, J.D., Bennett, D.L.H., Schwartz, A., et al. (2013). $\alpha 2\delta$-1 gene deletion affects somatosensory neuron function and delays mechanical hypersensitivity in response to peripheral nerve damage. J. Neurosci. *33*, 16412–16426. https://doi.org/10.1523/JNEUROSCI.1026-13.2013.
56. Li, C., Lei, Y., Tian, Y., Xu, S., Shen, X., Wu, H., Bao, S., and Wang, F. (2019). The etiological contribution of GABAergic plasticity to the pathogenesis of neuropathic pain. Mol. Pain *15*, 1744806919847366. https://doi.org/10.1177/1744806919847366.
57. Ferron, L., and Zamponi, G.,W. (2022). Voltage-Gated Calcium Channels in the Afferent Pain Pathway. In Voltage-Gated Calcium Channels, G.W. Zamponi and N. Weiss, eds. (Springer), pp. 491–514.
58. Brittain, J.M., Duarte, D.B., Wilson, S.M., Zhu, W., Ballard, C., Johnson, P.L., Liu, N., Xiong, W., Ripsch, M.S., Wang, Y., et al. (2011). Suppression of inflammatory and neuropathic pain by uncoupling CRMP-2 from the presynaptic Ca^{2+} channel complex.

Nat. Med. *17*, 822–829. https://doi.org/10.1038/nm.2345.

59. Li, L., Cao, X.H., Chen, S.R., Han, H.D., Lopez-Berestein, G., Sood, A.K., and Pan, H.L. (2012). Up-regulation of Cavβ3 subunit in primary sensory neurons increases voltage-activated Ca2+ channel activity and nociceptive input in neuropathic pain. J. Biol. Chem. *287*, 6002–6013. https://doi.org/10.1074/jbc.M111.310110.
60. Sun, L., Tong, C.K., Morgenstern, T.J., Zhou, H., Yang, G., and Colecraft, H.M. (2022). Targeted ubiquitination of sensory neuron calcium channels reduces the development of neuropathic pain. Proc. Natl. Acad. Sci. USA *119*, e2118129119. https://doi.org/10.1073/pnas.2118129119.
61. Honsek, S.D., Seal, R.P., and Sandkühler, J. (2015). Presynaptic inhibition of optogenetically identified VGluT3+ sensory fibres by opioids and baclofen. Pain *156*, 243–251. https://doi.org/10.1097/01.j.pain.0000460304.63948.40.
62. Arnot, M.I., Stotz, S.C., Jarvis, S.E., and Zamponi, G.W. (2000). Differential modulation of N-type 1B and P/Q-type 1A calcium channels by different G protein subunit isoforms. J. Physiol. *527*, 203–212. https://doi.org/10.1111/j.1469-7793.2000.00203.x.
63. Kupari, J., and Ernfors, P. (2023). Molecular taxonomy of nociceptors and pruriceptors. Pain *164*, 1245–1257. https://doi.org/10.1097/j.pain.0000000000002831.
64. Usoskin, D., Furlan, A., Islam, S., Abdo, H., Lönnerberg, P., Lou, D., Hjerling-Leffler, J., Haeggström, J., Kharchenko, O., Kharchenko, P.V., et al. (2015). Unbiased classification of sensory neuron types by large-scale single-cell RNA sequencing. Nat. Neurosci. *18*, 145–153. https://doi.org/10.1038/nn.3881.
65. Li, C.L., Li, K.C., Wu, D., Chen, Y., Luo, H., Zhao, J.R., Wang, S.S., Sun, M.M., Lu, Y.J., Zhong, Y.Q., et al. (2016). Somatosensory neuron types identified by high-coverage single-cell RNA-sequencing and functional heterogeneity. Cell Res. *26*, 83–102. https://doi.org/10.1038/cr.2015.149.
66. Zeisel, A., Hochgerner, H., Lönnerberg, P., Johnsson, A., Memic, F., van der Zwan, J., Häring, M., Braun, E., Borm, L.E., La Manno, G., et al. (2018). Molecular Architecture of the Mouse Nervous System. Cell *174*, 999–1014.e22. https://doi.org/10.1016/j.cell.2018.06.021.
67. Sharma, N., Flaherty, K., Lezgiyeva, K., Wagner, D.E., Klein, A.M., and Ginty, D.D. (2020). The emergence of transcriptional identity in somatosensory neurons. Nature *577*, 392–398. https://doi.org/10.1038/s41586-019-1900-1.
68. Dubin, A.E., and Patapoutian, A. (2010). Nociceptors: the sensors of the pain pathway. J. Clin. Invest. *120*, 3760–3772. https://doi.org/10.1172/JCI42843.
69. Liu, D.L., Lu, N., Han, W.J., Chen, R.G., Cong, R., Xie, R.G., Zhang, Y.F., Kong, W.W., Hu, S.J., and Luo, C. (2015). Upregulation of Ih expressed in IB4-negative Aδ nociceptive DRG neurons contributes to mechanical hypersensitivity associated with cervical radiculopathic pain. Sci. Rep. *5*, 16713. https://doi.org/10.1038/srep16713.
70. Berridge, M.J., Bootman, M.D., and Roderick, H.L. (2003). Calcium signalling: dynamics, homeostasis and remodelling. Nat. Rev. Mol. Cell Biol. *4*, 517–529. https://doi.org/10.1038/nrm1155.
71. Scheff, N.N., Lu, S.G., and Gold, M.S. (2013). Contribution of endoplasmic reticulum Ca2+ regulatory mechanisms to the inflammation-induced increase in the evoked Ca2+ transient in rat cutaneous dorsal root ganglion neurons. Cell Calcium *54*, 46–56. https://doi.org/10.1016/j.ceca.2013.04.002.
72. Scheff, N.N., and Gold, M.S. (2015). Trafficking of Na+/Ca2+ exchanger to the site of persistent inflammation in nociceptive afferents. J. Neurosci. *35*, 8423–8432. https://doi.org/10.1523/JNEUROSCI.3597-14.2015.
73. Yilmaz, E., Watkins, S.C., and Gold, M.S. (2017). Paclitaxel-induced increase in mitochondrial volume mediates dysregulation of intracellular Ca. Cell Calcium *62*, 16–28. https://doi.org/10.1016/j.ceca.2017.01.005.
74. D'Arco, M., Margas, W., Cassidy, J.S., and Dolphin, A.C. (2015). The upregulation of α2δ-1 subunit modulates activity-dependent Ca2+ signals in sensory neurons. J. Neurosci. *35*, 5891–5903. https://doi.org/10.1523/JNEUROSCI.3997-14.2015.
75. Wei, D., Mei, Y., Xia, J., and Hu, H. (2017). Orai1 and Orai3 Mediate Store-Operated Calcium Entry Contributing to Neuronal Excitability in Dorsal Root Ganglion Neurons. Front. Cell. Neurosci. *11*, 400. https://doi.org/10.3389/fncel.2017.00400.
76. Zheng, Y., Liu, P., Bai, L., Trimmer, J.S., Bean, B.P., and Ginty, D.D. (2019). Deep Sequencing of Somatosensory Neurons Reveals Molecular Determinants of Intrinsic Physiological Properties. Neuron *103*, 598–616.e7. https://doi.org/10.1016/j.neuron.2019.05.039.
77. Wang, F., Bélanger, E., Côté, S.L., Desrosiers, P., Prescott, S.A., Côté, D.C., and De Koninck, Y. (2018). Sensory Afferents Use Different Coding Strategies for Heat and Cold. Cell Rep. *23*, 2001–2013. https://doi.org/10.1016/j.celrep.2018.04.065.
78. MacDonald, D.I., Sikandar, S., Weiss, J., Pyrski, M., Luiz, A.P., Millet, Q., Emery, E.C., Mancini, F., Iannetti, G.D., Alles, S.R.A., et al. (2021). A central mechanism of analgesia in mice and humans lacking the sodium channel Na. Neuron *109*, 1497–1512.e96. https://doi.org/10.1016/j.neuron.2021.03.012.

STAR★METHODS

KEY RESOURCES TABLE

REAGENT or RESOURCE	SOURCE	IDENTIFIER
Antibodies		
Mouse anti-CGRP Ab	Abcam	Cat# Ab81887
Rabbit anti-GFP Ab	Abcam	Cat# Ab290
IB4-AF647	Thermo Fischer Scientific	Cat# I32450
Donkey anti-rabbit AF488	Thermo Fischer Scientific	Cat# A32790; RRID: AB_2535792
Donkey anti-mouse AF594	Thermo Fischer Scientific	Cat# A21203; RRID AB_141633
Rabbit anti-Trpv1 Ab	Alomone Labs	Cat# ACC-030
Mouse anti-GFP Ab	Abcam	Cat# 1218
Donkey anti-mouse AF488	Thermo Fischer Scientific	Cat# A32766; RRID AB_2762823
Donkey anti-rabbit AF647	Thermo Fischer Scientific	Cat# A31573; RRID AB_ 2536183
Biotin-conjugated goat anti-mouse Fab fragment	Jackson Immuno Research Lab	Cat# 115-067-003
Goat anti-mouse Fab IgG	Jackson Immuno Research Lab	Cat# 115-007-003
Streptavidin-AF 594	Thermo Fischer Scientific	Cat# S11227
Mouse monoclonal anti-dihydropyridine receptor antibody (α2 subunit)	Millipore-Sigma	Cat# D219
Chemicals, peptides, and recombinant proteins		
ω-Conotoxin GVIA	Alomone labs	Cat# C-300
ω-Agatoxin IVA	Alomone labs	Cat# STA-500
Baclofen	Millipore-Sigma	Cat# B5399
Tetrodotoxin	Alomone labs	Cat# T-550
Critical commercial assays		
Cacna1B ELISA kit	MyBioSource	Cat# MBS455655
Cacna1A ELISA kit	MyBioSource	Cat# MBS2887113
Experimental models: Organisms/strains		
Mouse: Trpv1cre B6.129-Trpv1tm1(cre)Bbm/J	The Jackson Laboratory	Stock # 017769
Mouse: Ai96 (RCL-GCaMP6s)	The Jackson Laboratory	Stock # 024106
Software and algorithms		
ThorImage®LS v4.1	Thorlabs	https://www.thorlabs.com
ImageJ	NIH	https://imagej.nih.gov/ij/
GraphPad Prism 9.0	GraphPad Software	https://www.graphpad.com/
LASX	Leica	https://www.leica-microsystems.com/

RESOURCE AVAILABILITY

Lead contact

Further information and requests for resources should be directed to and will be fulfilled by the lead contact, Gerald W. Zamponi (zamponi@ucalgary.ca).

Materials availability

This study did not generate new unique reagents.

Data and code availability

- All datasets reported in this work are available from the lead contact upon request.
- This paper does not report original code.
- Any additional information required to reanalyse the data reported in this paper is available from the lead contact upon request.

EXPERIMENTAL MODEL AND STUDY PARTICIPANT DETAILS

Mouse breeding

All experiments were carried out following approval of an animal protocol by the Institutional Animal Care and Use Committee at the University of Calgary. Mice were housed at a maximum of five per cage (30 × 20 × 15 cm) at 23 ± 1°C on a 12h-light:dark cycle (lights on at 7:00 a.m.) with *ad libitum* access to food and water. Homozygous Trpv1-Cre mice (Jax 017769) were purchased from The Jackson Laboratory. The Ai96 mice (Jax 024106) were provided by Dr. G. R. Gordon (University of Calgary) and bred at the University of Calgary Animal Resource Center. An in-house breeding program was used to generate Trpv1-GaMP6s mice by crossing the Trpv1cre driver mouse line with Ai96 conditional allele mice. Only male mice aged 6–12 weeks old were used in all experiments.

METHOD DETAILS

Spared nerve injury surgeries

SNI surgeries were performed on Trpv1-GCaMP6s mice. Under isoflurane anesthesia a 1 cm skin incision was made on the left thigh followed by a blunt dissection of the underlying muscles to expose the three branches of the sciatic nerve (common peroneal, tibial and sural nerves). Common peroneal and tibial nerves were tightly ligated with a silk suture (6-0, Ethicon, USA) and transected together. A 1 mm-long piece of the nerves was removed downstream the ligature. The thigh muscles and the skin were separately closed using sutures (6-0 silk and 4-0 Vicryl sutures, respectively). In Sham operated animals, the ligation and the transection of the nerves were omitted. Animals were tested for mechanical hyperalgesia 14 days after the surgery using a digital plantar aesthesiometer (UgoBasile, Varese, Italy) as previously described.[27] Briefly, animals were placed individually in testing chambers above a grid platform. The touch stimulator was placed underneath the grid platform allowing the filament to be positioned under the plantar surface of the hind paw of the animal. Each paw was tested three times. SNI animals that did not exhibit a neuropathic phenotype were discarded without further experiments.

Immunohistochemistry

Mice were anesthetized with isoflurane and transcardially perfused first with ice-cold PBS with heparin (20 U/mL), followed by 4% PFA/PBS. The spinal cord and lumbar L4 DRGs were dissected and post-fixed for 2 h with 4% PFA/PBS at room temperature and then transferred to 30% sucrose/PBS at 4°C for 48 h. The lumbar part of the spinal cord and the ganglia were frozen in OCT on dry ice and then sectioned (40 μm) using a cryostat (Leica CM3050 S). Samples were washed 3 times in PBS, blocked and permeabilized in 3% normal donkey serum with 0.3% Triton X-100 PBS for 90 min. Primary antibodies were incubated overnight in blocking solution at room temperature (mouse anti-CGRP Ab, 1:1000, ab81887, Abcam; rabbit anti-GFP Ab, 1:500, ab290, Abcam; IB4-AF647 1:250, ThermoFisher Scientific; mouse anti-GFP, 1:500, ab1218, Abcam; Rabbit anti-Trpv1 Ab, 1:250, ACC-030, Alomone Labs). After 3 washes in PBS, secondary antibodies were incubated for 3 h at room temperature (donkey anti-rabbit AF488, 1:500, A32790, and donkey anti-mouse AF594, 1:1000, A21203, ThermoFisher Scientific; donkey anti-mouse AF488, 1:1000, A32766, ThermoFisher Scientific; donkey anti-rabbit AF647, 1:500, A31573, ThermoFisher Scientific). Slices were washed twice in PBS before being incubated with DAPI (1:1000) in PBS for 10 min at room temperature. Slices were washed in PBS and in distilled water and mounted on glass slides to dry overnight and finally covered with Fluoromount/Plus (Cedarlane). Some sections were labeled for $Ca_V\alpha2$-δ-1 as previously described.[25] Briefly, after heat-induced epitope retrieval (10 mM citrate buffer, pH 6.0, 0.05% Tween 20, 95°C for 10 min), the sections were washed, blocked with 10% goat serum in PBS containing 0.3% Triton and the unconjugated goat Fab anti-mouse IgG (H + L) (0.1 mg/mL) for 1 h at RT. Mouse monoclonal anti-dihydropyridine receptor antibody (α2 subunit, Millipore-Sigma, 1:100) was applied for 2–3 days at 4°C. After 4 washes, the samples were incubated with biotin-conjugated goat anti-mouse Fab fragment (1:500, Jackson Immuno Research Lab) overnight at 4°C, followed by washes and streptavidin-AlexaFluor-594 overnight at 4°C (1:500, ThermoFisher Scientific). Images (1024 × 1024 pixels – optical section 0.7 μm) were acquired with LASX software driving a Leica TCS SP8 Laser Confocal microscope equipped with a 20 × 0.75 NA objective lens.

$Ca_V2.1$ and $Ca_V2.2$ protein quantification

Dorsal root ganglia were dissected from Sham and SNI animals (L4 ipsilateral side). Sample were homogenized in phosphate-buffered saline with complete protease inhibitor cocktail (Sigma-Millipore) and subjected to 4 freeze-thaw cycles. The samples were then centrifuged at 10,000 g for 10 min. The total protein concentration in the supernatant was quantified using the BCA method. Ten micrograms of total protein were used to determine $Ca_V2.X$ channel concentration using ELISA following the manufacturer's instructions (mouse Cacna1A and mouse Cacna1B, MyBioSource, San Diego, CA).

2-Photon microscopy

Anesthetized Trpv1-GCaMP6s mice were transcardially perfused with ice-cold sucrose aCSF (in mM: NaCl 125, KCl 3, $NaHCO_3$ 26, NaH_2PO_4 1.25, $MgCl_2$ 6, glucose 10, sucrose 252, pH7.35, bubbled with 5% CO_2/95% O_2). The spinal cord was dissected with lumbar (L3 to L5) dorsal roots intact and the dura removed. The spinal cord was incubated in aCSF (in mM: NaCl 125, KCl 3, $MgCl_2$ 1, $CaCl_2$ 2, $NaHCO_3$ 26, NaH_2PO_4 1.25, glucose 20, pH 7.35, bubbled with 5% CO_2/95% O_2) at room temperature for at least 1 h before imaging. The spinal cord was transferred into a custom 3D-printed imaging chamber and perfused with aCSF at 22 °C at a rate of 2.8 mL/min. A Bergamo II (Thorlabs, B242) articulated two-photon microscope was used with a tunable femtosecond Ti:Sapphire laser (Tiberius, Thorlabs). GCaMP6s was excited through a 25×/1.1-NA objective (Nikon, MRD77220) with the laser tuned to 920 nm and delivered to the sample via a primary longpass dichroic, separating the 920 nm 2P excitation from the visible emission light (690 nm, custom LP, Thorlabs) and the returned emitted light diverted through two secondary longpass dichroics(562 nm, FF562-Di03, Semrock, and 480 nm, DM480, Thorlabs) and an emission filter (FF03-525/50-25, Semrock) before reaching a GaAsP PMT (Thorlabs 2100 series). The L4 dorsal root was stimulated with a suction electrode connected to a constant current stimulator (DS3, Digitimer). Five hundred μs pulses were applied with variable intensity (from 0.1 to 30 mA). Images were acquired with ThorImageLS v4.1 software at either 2 frames per second on 1024 × 1024 pixel field of view (534.54 × 534.54 μm) or 30 frames per second on 512 × 256 pixel field of view (534.54 × 267.27 μm). At the end of each recording session, a z stack image of the dorsal horn was acquired to estimate the depth of the different fields of view. Images were analyzed in ImageJ using the Time Series Analyzer plugin (https://imagej.nih.gov/ij/plugins/time-series.html). For superficial dorsal horn imaging, the ImageJ-free hand tool was used to create a region of interest around fibers responding to electrical stimulation, and 5-pixel diameter circular ROIs were placed around responding varicosities in deeper layers of the dorsal horn. At least 10 ROIs were averaged for each animal. Peak fluorescence was determined by averaging 5–10 points of the plateau phase and subtracting the average of 10 points of the baseline before stimulation. Signal were expressed as ΔF/F0.

Drugs and toxins:GVIA (1 μM, Alomone labs), ω-Agatoxin IVA (200 nM, Alomone labs), Baclofen (100 μM, Millipore-Sigma), TTX (1 μM, Alomone labs), $CdCl_2$ (100 μM, Millipore-Sigma).

QUANTIFICATION AND STATISTICAL ANALYSIS

Data were analyzed with GraphPad Prism 9. Data are presented as the mean ± SEM. For box and whisker plots, boxes represent lower and upper quartile values, the bar represents the median, the whiskers represent the minimum and maximum data values. Unpaired t tests were used for comparison. Statistical significance was set at $p < 0.05$.